Thermodynamic Analysis of Human Plasma Apolipoprotein C-1: High-Temperature Unfolding and Low-Temperature Oligomer Dissociation†

Olga Gursky* and David Atkinson

Department of Biophysics, Boston University School of Medicine, 715 Albany Street, Boston, Massachusetts 02118

Received July 24, 1997; Revised Manuscript Received October 14, 1997

ABSTRACT: Thermal and chemical unfolding of lipid-free apolipoprotein C-1 (apoC-1), a 6-kDa protein component of very low density and high-density lipoproteins, was analyzed by far-UV CD. In neutral 1 mM Na_2HPO_4 solutions containing 6−7 μg/mL protein, the apoC-1 monomer is ∼30% α-helical at 0−22 °C and unfolds reversibly from about 22−80 °C with $T_m = 51 \pm 3$ °C and van't Hoff enthalpy $\Delta H_v(T_m) = 19 \pm 3$ kcal/mol. The apparent free energy of the monomer stabilization determined from the chemical unfolding at 0 °C, $\Delta G(0\ °C) = 2.8 \pm 0.8$ kcal/mol, decreases by about 1 kcal/mol upon heating to 25 °C. A small apparent heat capacity increment suggests the absence of a substantial hydrophobic core for the apoC-1 molecule. At pH 7, increasing apoC-1 concentration above 10 μg/mL leads to self-association and formation of additional α-helices that unfold upon both heating and cooling from room temperature. The CD data indicate that the high-temperature transition reflects a complete monomer unfolding and the low-temperature transition reflects oligomer dissociation into stable monomers. This suggests the importance of hydrophobic interactions for apoC-1 self-association. Close proximity between the high- and low-temperature transitions and the absence of a plateau in the chemical unfolding curves recorded from oligomeric apoC-1 indicate marginal oligomer stability and suggest that in vivo apoC-1 transfer is mediated via the complexes with other apolipoproteins and/or lipids.

Human plasma apolipoprotein C-1 (M_r = 6.605, 57 residues) is the smallest of the exchangeable apolipoproteins; it constitutes about 10% and 2% of the protein content in very low density lipoproteins (VLDL)[1] and high-density lipoproteins (HDL), respectively, and it is found in significant proportions on chylomicrons (*1*, *2*). ApoC-1 rapidly transfers among different lipoprotein classes, thereby altering their metabolic properties and playing a potentially important role in lipoprotein metabolism (*3*, *4*). The ability of apoC-1 to activate lecithin:cholesterol acyltransferase (LCAT) (*5*) has been suggested to account for normal plasma levels of cholesterol esters in subjects with deficiencies of the major LCAT activator, apolipoprotein A-1 (reviewed in ref *6*). In addition, apoC-1 has been shown to delay the clearance of potentially atherogenic triglyceride-rich lipoproteins (*7*), such as β-VLDL, by displacing apolipoprotein E or altering its conformation, thereby inhibiting β-VLDL uptake via the apoE-mediated LDL receptor-related pathway (*8*, *9*). The mechanisms of apoC-1 exchange among different lipoprotein classes are not clearly understood. In vitro studies indicate that apoC proteins may be transferred as complexes containing apoC-2, apoC-3, phospholipids and cholesterol, but the involvement of apoC-1 is not clear (reviewed in ref *2*). Alternatively, the transfer of apoC-1 may be mediated via the water-soluble lipid-poor or lipid-free species and may be controlled or even regulated by the conformation of these species in plasma (*10*, *11*). Few details are available on the solution conformation and stability of lipid-free apoC-1, which is the focus of this work.

Amino acid sequence analysis of apoC-1 suggests the presence of four 11-residue tandem repeats that may form two class-A amphiphatic α-helices spanning residues 7−32 and 33−53 (*12*). Such helices, characterized by a specific distribution of charged and hydrophobic groups, have been predicted on the basis of the sequences of other exchangeable apolipoproteins and are proposed to account for their lipid-binding affinity (*12*). Long amphiphatic α-helices packed in five- or four-helix bundles have been observed in the X-ray crystal structures of locust apolipoprotein Lp-3 (*13*) and the N-terminal domain of human apoE (*14*). Preliminary X-ray diffraction data recorded from apoC-1 crystals is also consistent with end-to-end packing of elongated α-helix bundles (*15*). Furthermore, NMR studies of the peptides corresponding to the proposed lipid-binding regions of apoC-1 indicate that, in the presence of the lipid-mimicking solvent sodium dodecyl sulfate (SDS), these peptides adopt amphiphatic α-helical conformations (ref *16* and references therein).

Similar to other exchangeable apolipoproteins, apoC-1 shows a substantial increase in the α-helical content upon lipid binding (reviewed in ref *10*). Furthermore, far-UV CD and sedimentation studies have shown that self-association of apoC-1 with increasing protein concentration from 0.01

† This work was aided by Grant 13-512-956 from the American Heart Association, Massachusetts Affiliate, to O.G. and by NIH Grant HL26335 to D.A.

* Corresponding author. FAX: (617)-638-4041. Phone: (617)-638-4207. E-mail: gursky@med-biophd.bu.edu.

[1] Abbreviations: apo, apolipoprotein; HDL, high-density lipoprotein; LDL, low-density lipoprotein; VLDL, very low density lipoprotein; LCAT, lecithin:cholesterol acyltransferase; UV, ultraviolet; CD, circular dichroism; Gdm Cl, guanidine hydrochloride; SDS, sodium dodecyl sulfate.

S0006-2960(97)01801-1 CCC: $15.00
Published on Web 01/06/1998

to 2.8 mg/mL at pH 7 and 25 °C leads to an unusually large increase in the α-helical content from about 33% to 80% (*10*, *17*). This α-helical structure was proposed to have low stability, on the basis of the absence of a plateau at low guanidine hydrochloride (Gdm Cl) concentrations in the chemical unfolding curve recorded from 0.2 mg/mL apoC-1 (*17*). No quantitative analysis of the chemical unfolding data and no data on the temperature dependence of the molecular properties of apoC-1 have been reported. Thus, the thermodynamic parameters for this apolipoprotein remain unknown.

Determining the thermodynamic parameters for lipid-free apoC-1 is important for understanding the energetic and structural basis for its conformational adaptability to the polar environment in plasma and to the apolar environment on lipoprotein particles of various sizes and compositions, and for assessing possible modes of in vivo apoC-1 transfer. Our recent thermodynamic analysis of exchangeable apolipoproteins A-1 and A-2 implicated a molten globular-like state for these lipid-free proteins in neutral low-salt solutions (*18*, *19*). The molten globule is a compact folding intermediate characterized by a well-defined near-native secondary structure, a lax nonspecific tertiary structure, a high propensity to self-associate, a binding affinity for small hydrophobic ligands, broad low-cooperativity thermal unfolding, and relatively low values of stabilization energy ΔG(25 °C), transition enthalpy ΔH, and heat capacity increment ΔC_p (*20*, *21*). Similarity between the physicochemical and functional properties of exchangeable apolipoproteins suggests that their lipid-free states may have molten globule-like structures. To determine which of the molten globular characteristics apply to apoC-1, we used CD spectroscopy to monitor thermal and Gdm Cl unfolding of human lipid-free apoC-1 over a broad range of temperatures (−10 to +95 °C), protein concentrations (6−220 μg/mL), and solvent ionic conditions (pH 3.7−7.5, 1−200 mM Na_2HPO_4). We report the observation and interpretation of apoC-1 unfolding upon heating and cooling from room temperatures, and carry out a quantitative thermodynamic analysis of apoC-1 monomer unfolding in neutral low-salt solutions. Such analysis may provide a better insight into the energetic-structure−function relationship of apoC-1 and serve as a model for larger apolipoproteins.

ApoC-1 was selected for this analysis for the following reasons: (i) it shows a large increase in the secondary structure upon self-association and lipid binding that can be accurately measured by CD; (ii) it has no glycosylation sites that may potentially complicate the thermodynamic and structural analysis; and (iii) it is the only intact human apolipoprotein that has been shown to form diffraction quality crystals, providing a potential for a future high-resolution structural−thermodynamic analysis.

EXPERIMENTAL PROCEDURES

Protein Isolation and Purification. ApoC-1, which was isolated and purified from human plasma HDL as described (*22*), migrated as a single band corresponding to $M_r \sim 6000$ on 10% SDS polyacrylamide gel. The protein was predissolved at ∼200 μg/mL in 6 M urea and refolded by dialysis against 2 M Gdm Cl and 10 mM phosphate buffer at pH 8, followed by an extensive dialysis against the appropriate buffer. The protein prepared by using this procedure has been shown to retain full biological activity (*22*). Protein and buffer solutions were filtered using a 0.45 Millipore filter. Protein concentrations were determined by a modified chromatographic Lowry assay (*23*) and by UV absorbance at 280 nm, which was facilitated by the presence of a single Trp41 residue in the apoC-1 sequence. The agreement between the concentrations measured prior to and following the CD experiments was better than 10%.

Circular Dichroism Spectroscopy. Far-UV CD spectra (190−250 nm) were recorded with an AVIV 62DS spectrophotometer (AVIV Associates, Inc.) equipped with a thermoelectric temperature control and calibrated with d_{10}-camphorsulfonic acid. The spectra were recorded from protein solutions of 6−220 μg/mL concentrations in 10-0.5-mm quartz cuvettes, depending on the concentration. The spectra were recorded with a 1−1.5 nm bandwidth, and a 0.5 nm step size at a rate of 2 nm/s and averaged over 3−5 runs. The ellipticity at 222 nm and/or other characteristic wavelengths (193, 198, 208, and 230 nm) was recorded as a function of temperature from −10 to +95 °C. Subzero temperatures were achieved by undercooling dust-free protein and salt solutions, in the absence of cryoprotectors. To ensure the equilibrium character of the thermal transitions, the ellipticity functions $\Theta(T)$ were recorded at several heating/cooling rates from 1.5 to 15 °C/h, with the time for recording a data point ranging from 15 to 99 s and the temperature step size from 0.5 to 0.3 °C, respectively. Chemical unfolding was carried out using a series of protein solutions containing 6.0−7.6 μg/mL apoC-1, 2 mM Na_2HPO_4, and varying concentrations of Gdm Cl (0−3 M). Urea unfolding experiments were not performed because of the tendency of apoC-1 to precipitate in the presence of moderate concentrations of urea. Prior to the CD measurements, the solutions were equilibrated at room temperature overnight. The CD data at 222 nm were taken from these solutions at 0 and 25 °C, with 5−15 min for recording a data point. The reversibility of the chemical unfolding of apoC-1 was confirmed by the ellipticity measurements upon dilution of 10 μg/mL protein solutions containing 0.8−1.6 M Gdm Cl. The buffer baselines were subtracted from the protein CD data that were subsequently normalized to the protein concentration and expressed as a mean residue ellipticity. The estimates of the α-helical content in apoC-1 at pH 7 using the ellipticity at 208 (*24*) and 222 nm (*25*) agreed within 2%. These estimates were in good agreement with the results of the secondary structural analysis based on deconvolution of the CD spectra recorded from monomeric apoC-1 at pH 7, which was carried out using the algorithm of Mao and Wallace (26) with the reference data sets from ref *25*. Equilibrium thermodynamic analysis of the thermal and chemical unfolding was carried out by conventional methods (*27*), by using the data recorded from 6 to 7.6 μg/mL apoC-1, 1 mM Na_2HPO_4 at pH 7.

RESULTS

Thermal Unfolding of ApoC-1 Monomer at pH 7. Far-UV CD data were recorded from protein solutions containing 6−7.6 μg/mL apoC-1, and 1−5 mM Na_2HPO_4 at pH 7−7.5. Since the molecular weight of apoC-1 in a near-neutral low-salt solution of 10 μg/mL protein concentration has been shown to approach that of the monomer (*17*), the protein is entirely monomeric under the conditions of these CD

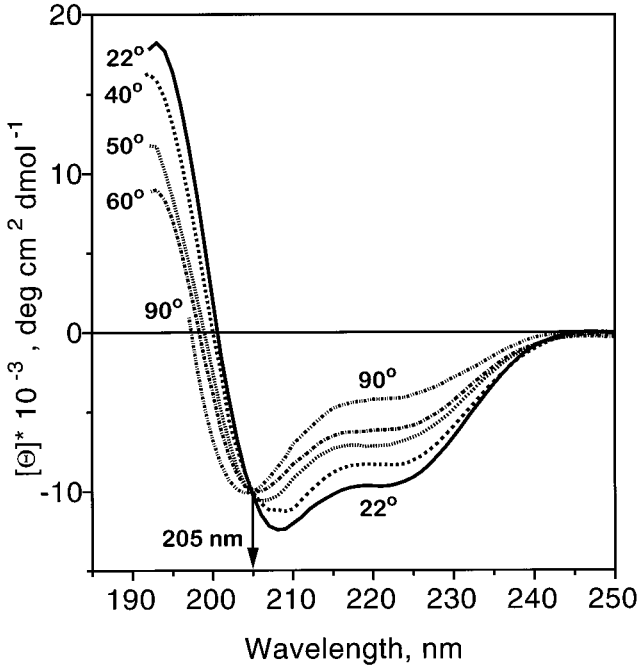

FIGURE 1: Far-UV CD spectra of monomeric apoC-1 at several constant temperatures and pH 7. The spectra were recorded from a solution of 7 μg/mL apoC-1 in 1 mM Na_2HPO_4; the temperatures are indicated on the lines. The spectra at 22 and 0 °C (not shown) significantly overlap. An isochromatic point at 205 nm is indicated by an arrow. The spectrum recorded at 90 °C (with the residual molar ellipticity $[\Theta_{222}] \sim 4 \times 10^3$ deg·cm^2·dmol^{-1}) is typical for the heat-unfolded proteins that are devoid of any detectable residual secondary structure (*28*, *31*).

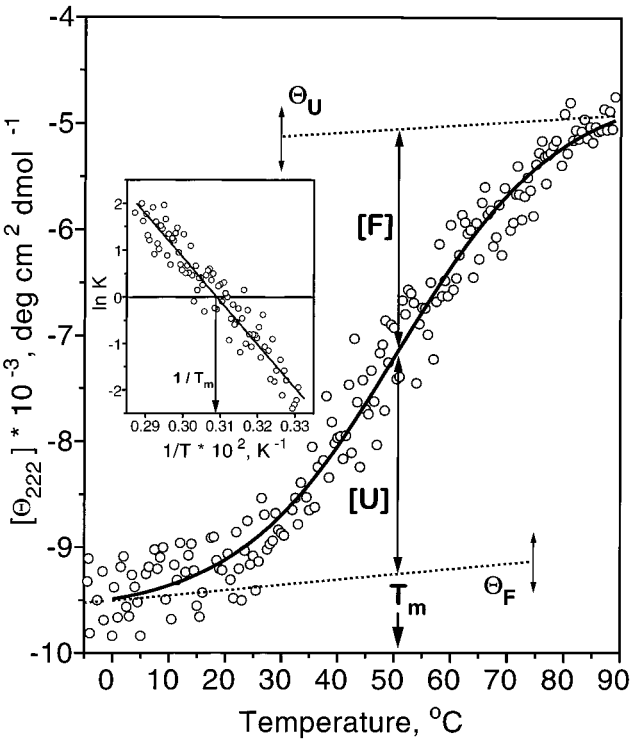

FIGURE 2: Thermal unfolding of monomeric apoC-1 at pH 7 monitored by CD at 222 nm. The data were recorded from a solution of 6.6 μg/mL apoC-1 in 1 mM Na_2HPO_4 upon heating from −5 to 90 °C. Ellipticity curve $\Theta_{222}(T)$. Data points are designated by circles, the solid curve illustrates the least-squares fit by a sigmoidal function ($\chi^2 = 0.068$), and the midpoint, $T_m = 51 \pm 0.9$ °C, of the sigmoidal fitting function is shown by an arrow. Dashed lines show the baselines for the folded Θ_F and unfolded Θ_U states that were used in the van't Hoff analysis, and long double arrows illustrate the proportions of the folded [F] and unfolded [U] states. Since the broad extent of apoC-1 unfolding precludes extensive ellipticity measurements outside the transition region, the slopes of the baselines $\Theta_F(T)$ and $\Theta_U(T)$ are not very well defined. Plausible baselines (indicated by short double arrows) range from temperature-independent functions that intercept the data outside the transition region to linear extrapolations of the short pre- and post-transitional regions of the data. The baselines used in the van't Hoff analysis are in the middle of this range. (Inset) Van't Hoff plot ln K versus $1/T$. The equilibrium constant $K(T) = [U(T)]/[F(T)] = [\Theta_F(T) - \Theta_{222}(T)]/[\Theta_{222}(T) - \Theta_U(T)]$, which was calculated using the data $\Theta_{222}(T)$ and the baselines $\Theta_F(T)$ and $\Theta_U(T)$ in the transition region (from 30 to 75 °C), is designated by circles; the solid line shows the least-squares approximation by a linear function (standard deviation of 0.36). The intercept of the linear function with the abscissa defines the midpoint $T_m = 50 \pm 3$ °C (shown by an arrow), and the slope provides the effective enthalpy $\Delta H_v(T_m) = -R$ [d ln K/d $(1/T)$] $= 19 \pm 3$ kcal/mol, where $R = 1.987$ cal/(mol·K) is the gas constant. The uncertainties in these estimates incorporate the fitting errors (±0.9 °C for T_m and ±0.75 kcal/mol for $\Delta H_v(T_m)$), the uncertainties in the baseline extrapolation, the deviations between the CD data recorded from different samples, and the deviations between the data recorded at 222 and 230 nm.

experiments. Figure 1 shows the CD spectra recorded at several constant temperatures from 0 to +90 °C, and Figure 2 shows the thermal unfolding upon heating from −5 to +90 °C monitored by ellipticity $\Theta_{222}(T)$ at 222 nm. These spectra indicate that the secondary structure is composed of 30% α-helix, ≤15% β-structure, and ≥55% random coil at 0−22 °C and unfolds above 22 °C.

The melting curves $\Theta_{222}(T)$ recorded at several different scanning rates from 1.5 to 15 °C/h superimpose completely, indicating the equilibrium character of the transition. Furthermore, the ellipticity at 22 °C was completely restored after heating to 70 °C followed by re-equilibration at 22 °C, which confirmed the reversibility of the thermal unfolding. Prolonged heating to higher temperatures followed by cooling to 22 °C led to about 10% reduction in the molar ellipticity at 22 °C. Similar irreversible spectral changes above 70 °C have been observed in apoA-1 (*18*) and in other proteins and peptides (*27*−*29*) and are probably linked to protein chemical modifications at high temperature (*28*). Since these irreversible changes are relatively slow compared to the protein heat unfolding, they do not preclude equilibrium thermodynamic analysis of the unfolding transition (*28*).

The spectra in Figure 1 have a well-defined isochromatic point, which is consistent with the presence of only two alternative conformations in the apoC-1 molecule. The sigmoidal shape of the melting curve $\Theta_{222}(T)$ in Figure 2 is indicative of cooperativity, but the broad extent of the transition (from about 22 to 80 °C) suggests that the cooperativity unit is relatively small. Van't Hoff analysis of the ellipticity function $\Theta_{222}(T)$ provides the midpoint temperature $T_m = 50 \pm 3$ °C and effective enthalpy $\Delta H_v(T_m)$ $= 19 \pm 3$ kcal/mol (Figure 2, insert). Similar values of T_m and $\Delta H_v(T_m)$ are obtained from the analysis of the ellipticity function $\Theta_{230}(T)$ recorded at 230 nm (data not shown). The errors in the estimates of T_m and $\Delta H_v(T_m)$ incorporate the uncertainty in the baseline extrapolations for the broad heat unfolding transition of apoC-1 (Figure 2) and the fitting errors in the approximation of the van't Hoff plot by a linear function that are relatively large because of the relatively low signal-to-noise ratio in the CD data recorded from low protein concentrations (Figure 2). As a result, the errors

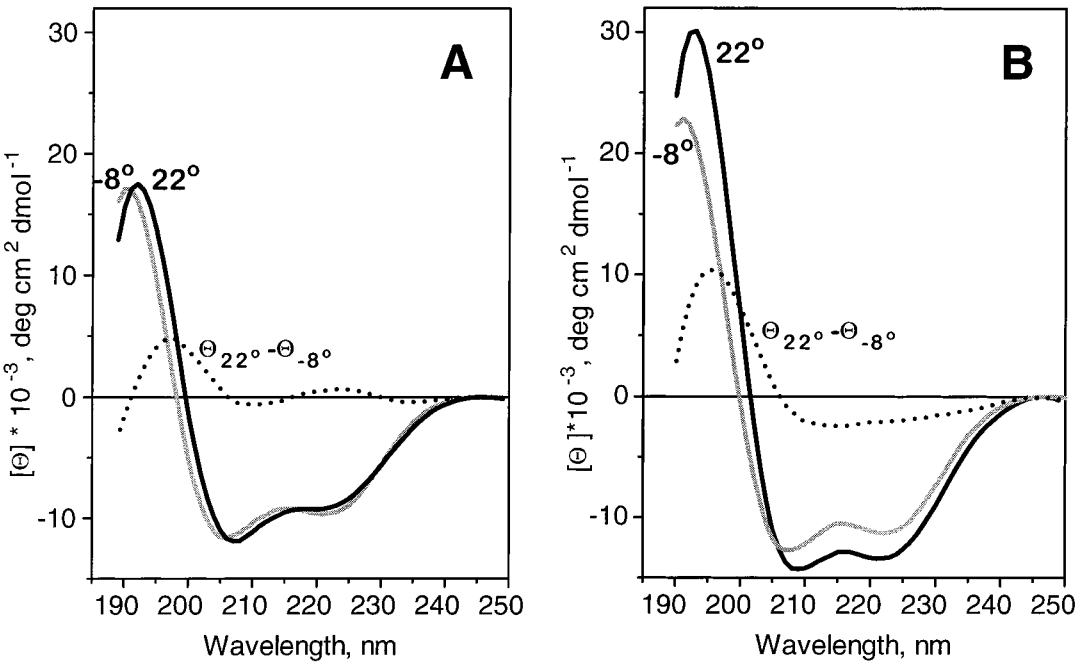

FIGURE 3: Comparison of the CD spectra recorded at 22 and −8 °C from neutral low-salt solutions of differing apoC-1 concentrations. Far-UV CD spectra at 22 °C (black lines) and at −8 °C (gray lines) were recorded from 1 mM Na_2HPO_4 solutions of (A) 10 μg/mL and (B) 200 μg/mL apoC-1 concentrations. Dotted lines show the difference spectra $[\Theta]_{22} - [\Theta]_{-8}$. In part A, cooling from 22 to −8 °C leads to only small 1−2-nm shifts in the CD bands, without any significant changes in the band intensities. In part B, cooling from 22 to −8 °C leads to a substantial reduction in the intensity of the positive CD band at ∼193 nm and the negative CD bands at 208 and 222 nm that are characteristic of the α-helical structure. The difference spectrum $[\Theta]_{22} - [\Theta]_{-8}$ that approximates the spectrum of the structure lost upon cooling indicates partial unfolding of the α-helical structure.

in the van't Hoff analysis of apoC-1 are comparable to those reported for the unfolding of the α-helical peptides (*29*) but are relatively large compared to the uncertainties in T_m (±0.5 °C) and $\Delta H_v(T_m)$ (5−10%) reported for typical globular proteins (*27*).

The van't Hoff enthalpy ΔH_v experimentally determined from the CD data in Figure 2 can be compared to the predicted calorimetric enthalpy ΔH_{cal} of unfolding of the α-helical portion of the apoC-1 molecule that is composed of ∼30% of the protein, or ∼17 amino acids. The predicted enthalpy is $\Delta H_{cal} = 17-22$ kcal/(mol·K), using the values 1.0−1.3 kcal/(mol·K) measured for the helix-to-coil transition of the α-helical peptides in water (*29*). The agreement between ΔH_v and ΔH_{cal}, within the error of their estimates, suggests that the size of the cooperative unit in apoC-1 is comparable to the number of groups forming the α-helical structure (∼17 residues).

Effect of Protein Concentration on the Thermal Unfolding. Figure 3 shows the CD spectra recorded at 22 and −8 °C from solutions containing 10 μg/mL and 200 μg/mL apoC-1 in 1 mM Na_2HPO_4 at pH 7, and Figure 4 shows the melting curves $\Theta_{222}(T)$ recorded from −10 to +95 °C from apoC-1 solutions of 20, 100, and 220 μg/mL concentrations at pH 7. Comparison of the spectra recorded at 22 °C (black lines in Figure 3 A,B) and the melting curves 2−4 in Figure 4 shows that increasing apoC-1 concentration from 10 to 220 μg/mL in neutral low-salt solutions leads to a progressive increase in the protein α-helical content from about 30% to 42%. This observation agrees with the earlier report on apoC-1 self-association that was detected at >10 μg/mL apoC-1, pH 7, 25 °C and was accompanied by an increase in the protein α-helical content (*17*). Furthermore, the melting curves 2−4 show small high-temperature shifts with increasing protein concentration. Such shifts are characteristic of the thermal unfolding accompanied by oligomer dissociation and are a consequence of the Le Chatelier principle, according to which increasing protein concentration should shift the equilibrium toward the folded oligomeric protein state (*30*). Thus, the observed shifts in the melting curves 2−4 are consistent with the known self-association properties of apoC-1 and are not indicative of an increased thermal stability of the oligomeric protein.

In contrast to the melting curves recorded from 6.0−7.6 μg/mL apoC-1 solutions (Figure 2), the ellipticity curves 2−4 in Figure 4 recorded from 20−220 μg/mL apoC-1 show that the α-helical structure is maximal at about 22 °C and unfolds not only upon heating but also upon cooling from room temperature. Coincident ellipticity changes observed at different wavelengths and the sigmoidal shapes of the unfolding curves above and below 22 °C (Figure 4, inset) suggest some cooperativity for both the high- and low-temperature transitions. A complete overlap of the ellipticity curves measured from identical samples at different heating/cooling rates indicates that the transitions are fully reversible in the temperature range from −10 to 70 °C. Comparison of the unfolding curves 2−4 suggests that the low-temperature transition becomes more pronounced at higher protein concentrations (100−220 μg/mL). This trend is also apparent from the comparison of the CD spectra in Figure 3. Figure 3A shows that cooling from 22 to −8 °C leads to only small (<2 nm) shifts in the positions of the characteristic CD bands recorded from 10 μg/mL apoC-1, without any significant changes in the band intensities (Figure 3A). Such spectral shifts are characteristic of the temperature-dependent solvent effects and may lead to nonzero slopes in the ellipticity functions recorded at constant wavelengths in the pre- and

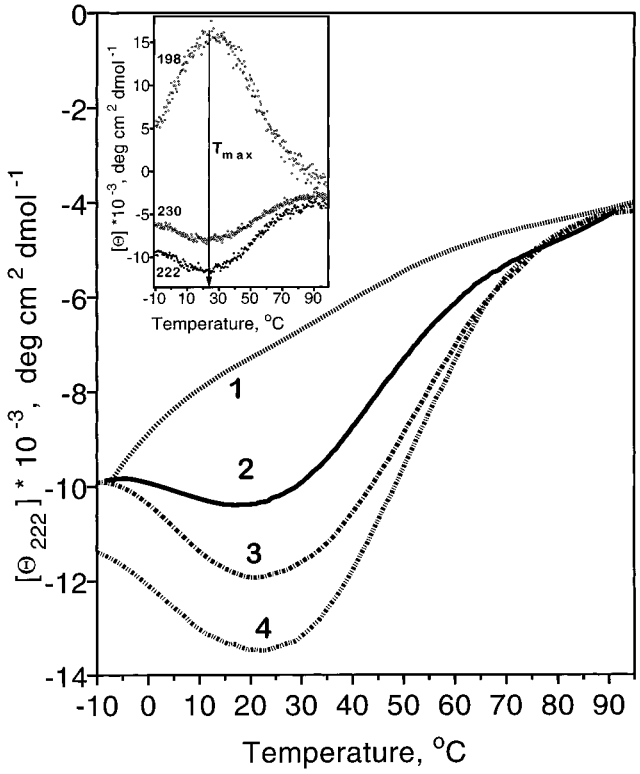

FIGURE 4: Thermal unfolding of apoC-1 in low-salt solutions of different pH and protein concentrations monitored by CD at 222 nm. The numbers on the curves indicate the following experimental conditions: (1) 160 μg/mL apoC-1, 5 mM acetate buffer, pH 3.7; (2) 20 μg/mL apoC-1, 1 mM Na_2HPO_4, pH 7; (3) 100 μg/mL apoC-1, 1 mM Na_2HPO_4, pH 7; (4) 220 μg/mL apoC-1, 1 mM Na_2HPO_4, pH 7. Inset: Raw data showing thermal unfolding of apoC-1 monitored at 198, 222, and 230 nm (the wavelengths are indicated on the curves). The sample conditions are identical to those of curve 3 (100 μg/mL apoC-1, pH 7). The arrow shows the temperature $T_{max} \sim 22$ °C of the maximal α-helical content. The nearly 3-fold reduction in the noise level in the melting curve $\Theta_{222}(T)$ compared to that in Figure 2 is due to a 10-fold increase in apoC-1 concentration used to record this curve. Fitting of the low-temperature portion of the $\Theta_{222}(T)$ data (−10 to 22 °C) by a sigmoidal function ($\chi^2 = 0.01$) is significantly more accurate than the linear approximation ($\chi^2 = 0.02$), suggesting some cooperativity for the low-temperature transition.

posttransitional regions (such as the baselines Θ_F and Θ_U in Figure 2). In contrast, a similar cooling of the apoC-1 solution of 220 μg/mL concentration leads to a significant reduction in the intensities of the peptide CD bands that are characteristic of the α-helical content in "all-α" proteins (*24*, *25*) (Figure 3B). The observed ∼25% reduction in the positive ellipticity at 193 nm and ∼15% reduction in the negative ellipticity at 208 and 222 nm are indicative of a reduction in the α-helical content of apoC-1 from about 41% to 36% upon cooling from 22 to −8 °C. Furthermore, the data in Figure 4 demonstrate that the substantial molar ellipticity $\Theta_{222}(-10\ °C) \leq -10\,000$ deg·cm²·dmol⁻¹ corresponding to ≥30% α-helical content is retained at −10 °C when the low-temperature transition is apparently close to completion. In contrast, heat unfolding leads to a complete disruption of the α-helical structure in apoC-1, as indicated by the CD spectrum recorded at 90 °C (Figure 1) that is characteristic of the random coil conformation, and the residual molar ellipticity $\Theta_{222}(90°) = -4500$ observed upon completion of the high-temperature unfolding (Figures 2 and 4) that is typical for completely heat unfolded proteins

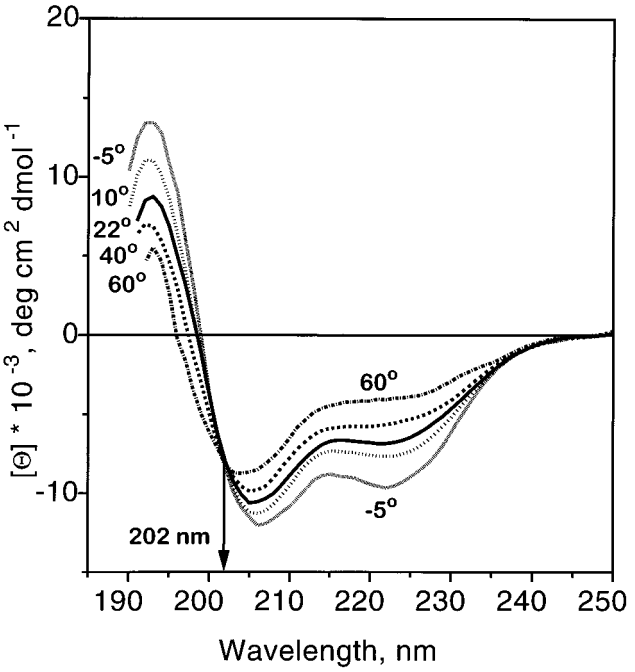

FIGURE 5: Far-UV CD spectra of apoC-1 at several constant temperatures and pH 3.7. The spectra were recorded from 100 μg/mL apoC-1 in 5 mM $NaC_2H_3O_2$ buffer. The temperatures are indicated on the lines. A small but significant 3-nm shift in the position of the isochromatic point at 202 nm (shown by an arrow) compared to that at pH 7 (Figure 1) indicates protein conformational changes in this pH range.

(*28*). Thus, the low-temperature transition leads to only partial unfolding of the α-helical structure in apoC-1, whereas the high-temperature transition leads to a complete protein unfolding.

Effects of pH, Salt, and Denaturant on the High- and Low-Temperature Transitions. CD spectra and the thermal unfolding curves were recorded from 7−220 μg/mL apoC-1 solutions in 1−5 mM phosphate buffer at pH 6.5−8 and in 5 mM acetate buffer at pH 3.7. The CD data recorded at pH 6.5, 7, and 8 under otherwise identical conditions completely superimpose, suggesting that the secondary structure and stability of apoC-1 are invariant in this pH range. In contrast, decreasing the pH from 7 to 3.7 leads to significant spectral changes that are indicative of a reduced α-helical content at room temperature (curve 1 in Figure 4, solid curves in Figures 1 and 5 compared). A small but significant 3-nm difference in the positions of the isochromatic points at pH 7 and 3.7 (Figures 1 and 5) is also consistent with the protein conformational changes occurring in this pH range. Furthermore, in contrast to sigmoidal ellipticity changes observed at near-neutral pH, the melting curve 1 in Figure 4 recorded at pH 3.7 shows only a gradual decrease in the α-helical content upon heating from −10 to 95 °C. In contrast to the CD data recorded at near-neutral pH, the molar ellipticity and the melting curves recorded at pH 3.7 are independent of apoC-1 concentration in the range explored. This is consistent with the earlier CD and sedimentation studies of apoC-1 that demonstrated the absence of self-association at acidic pH (*17*).

Figure 6 shows thermal unfolding curves recorded from 20 μg/mL apoC-1 solutions at pH 7.5 containing (1) 1 mM phosphate buffer, (2) 200 mM phosphate buffer, and (3) 0.2 M Gdm Cl in 1 mM phosphate. These curves suggest that

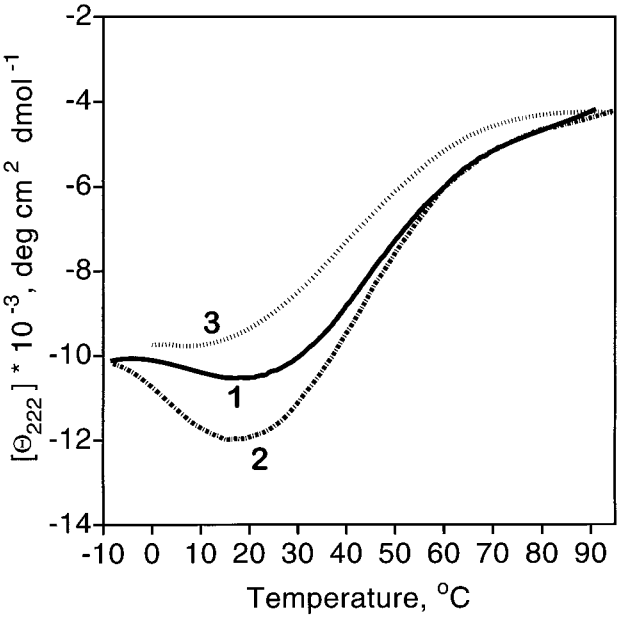

FIGURE 6: Effects of Na_2HPO_4 and Gdm Cl on the thermal unfolding of apoC-1. The melting curves were recorded at 222 nm from samples containing 20 μg/mL apoC-1 at pH 7−7.5. The numbers on the curves indicate the following solvent conditions: (1) 1 mM Na_2HPO_4 (similar to curve 2 in Figure 4); (2) 200 mM Na_2HPO_4; and (3) 1 mM Na_2HPO_4, 0.2 M Gdm Cl.

Na_2HPO_4 and Gdm Cl have opposite effects on the molar ellipticity and thermal unfolding of apoC-1. Increasing sodium phosphate concentration from 1 to 200 mM leads to a significant increase in the α-helical content at 22 °C indicated by a change in Θ_{222}(22 °C) from about −10 500 to −12 000 deg·cm^2·dmol^{-1} (curves 1 and 2 in Figure 6). Both high- and low-temperature unfolding transitions of this α-helical structure are readily detectable. In contrast, the ellipticity curve 3 in Figure 6 recorded in the presence of 0.2 M Gdm Cl indicates a significant reduction in the α-helical content of apoC-1 at 22 °C (Θ_{222}(22 °C) ∼ −9500). This α-helical structure unfolds upon heating, but shows no significant unfolding upon cooling from 22 °C.

Guanidine Hydrochloride Unfolding of Monomeric ApoC-1. Chemical unfolding data Θ_{222}([Gdm Cl]) were recorded at 0 and 25 °C from samples containing 6.0−7.6 μg/mL apoC-1 in 1 mM Na_2HPO_4 at pH 7.5 and varying Gdm Cl concentrations (Figure 7). The unfolding curve at 0 °C is sigmoidal (open symbols in Figure 7), with a narrow pretransitional region suggesting an appreciable stabilization energy. Linear approximation of the free energy as a function of Gdm HCl concentration, calculated using this data with the baselines $\Theta_{F,0°}$ and Θ_U obtained by linear extrapolation of the pre- and posttranslational regions (Figure 7), provides the transition midpoint [Gdm Cl]$_{1/2}$ ∼ 0.85 M; the extrapolation to 0 denaturant concentration provides the free energy of stabilization ΔG_{H_2O}(0 °C) = 2.8 ± 0.8 kcal/mol (Figure 7, inset). The error in this estimate incorporates the uncertainty in the baseline extrapolation for the folded state from the narrow pretransitional region and the fitting errors (which are relatively large because of the reduced signal-to-noise ratio in the data measured from low protein concentrations). Therefore, the accuracy in estimating the free energy of apoC-1 stabilization is lower than that reported for typical globular proteins (≤0.5 kcal/mol) (*27*).

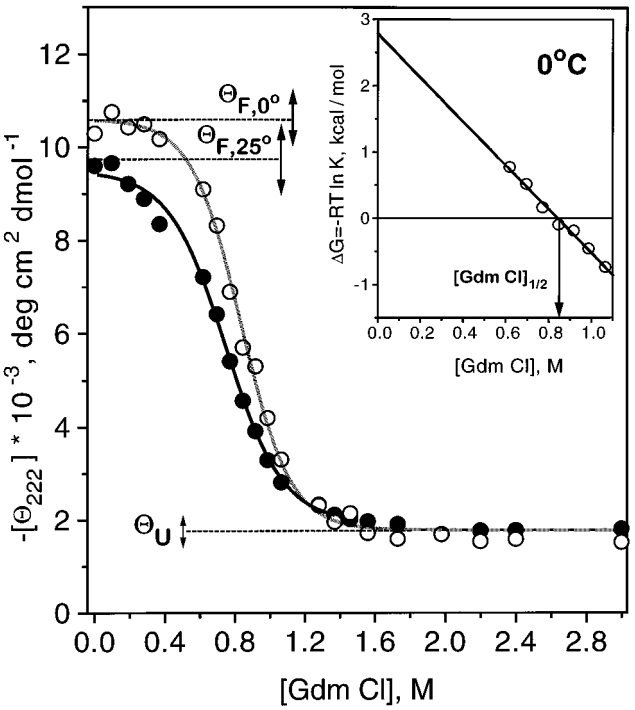

FIGURE 7: Gdm Cl unfolding of monomeric apoC-1 monitored by CD at 222 nm. The ellipticity data Θ_{222} were recorded from 7 μg/mL apoC-1 in 5 mM Na_2HPO_4, pH 7.5 at 0 °C (solid circles) and 25 °C (open circles). The gray solid line shows the fitting to the data at 0 °C by a sigmoidal function, with the midpoint of the sigmoidal fitting function [Gdm Cl]$_{1/2}$ = 0.84 ± 0.07 M indicated by an arrow. The black solid line illustrates sigmoidal fitting to the data at 25 °C. Dashed lines show the baselines $\Theta_{F,0}$, $\Theta_{F,25}$, and Θ_U for the folded and unfolded protein states at 0 and 25 °C, respectively, that were used to calculate the free energy of protein stabilization $\Delta G(0)$ and $\Delta G(25)$, and double arrows indicate the uncertainties in the baseline extrapolations. The residual ellipticity [Θ_{222}] ∼ 2 × 10^3 deg·cm^2·dmol^{-1} observed at >1.5 M Gdm Cl concentrations is typical for the fully unfolded α-helical proteins. Inset: Free energy of apoC-1 stabilization at 0 °C as a function of Gdm Cl concentration. Gibbs free energy ΔG([Gdm Cl]) = $-RT$ ln K (where K = [U]/[F] = ($\Theta_F - \Theta_{222}$)/($\Theta_{222} - \Theta_U$) is the equilibrium constant, R = 1.987 cal/(mol·K) is the gas constant, and T = 0 °C = 273.15 K), was calculated using the data points Θ_{222} at 0 °C in the transition region (open circles). Linear approximation of the free energy function ΔG([Gdm Cl]) = ΔG_{H_2O} + m[Gdm Cl] (solid line, standard deviation 0.07) provides the free energy of apoC-1 stabilization in the absence of Gdm Cl, $\Delta G_{H_2O}(0)$ = 3.1 ± 0.8 kcal/mol, the midpoint [Gdm Cl]$_{1/2}$ = 0.85 ± 0.1 M, and m = 3.7 ± 0.7 kcal/[mol(protein)·mol(Gdm Cl)]. The uncertainties in these estimates incorporate the fitting errors (±0.15 for ΔG_{H_2O}(0°), ±0.17 for m), the uncertainties in the baseline extrapolation for Θ_F from the narrow pretransitional region, and the deviations between the CD data recorded from different samples of 6.0−7.7 μg/mL apoC-1 concentrations at pH 7.5.

The GdmHCl unfolding curve at 25 °C is shifted to lower denaturant concentrations (curves in closed and open symbols in Figure 7 compared), suggesting reduced protein stability upon heating from 0 to 25 °C. This is consistent with the melting curve in Figure 2, which suggests that apoC-1 is fully folded at 0 °C but may be ∼10% unfolded at 25 °C. The pretransitional region in the chemical unfolding curve at 25 °C is insufficient to provide a reliable baseline extrapolation for the folded state. To estimate the upper limit of apoC-1 stability at 25 °C, we used a temperature-independent baseline $\Theta_{F,25°}$ that intercepts the data at 0 denaturant concentration; an estimate of the lower limit of ΔG_{H_2O}(25) was obtained by using a baseline $\Theta_{F,0°}$. The

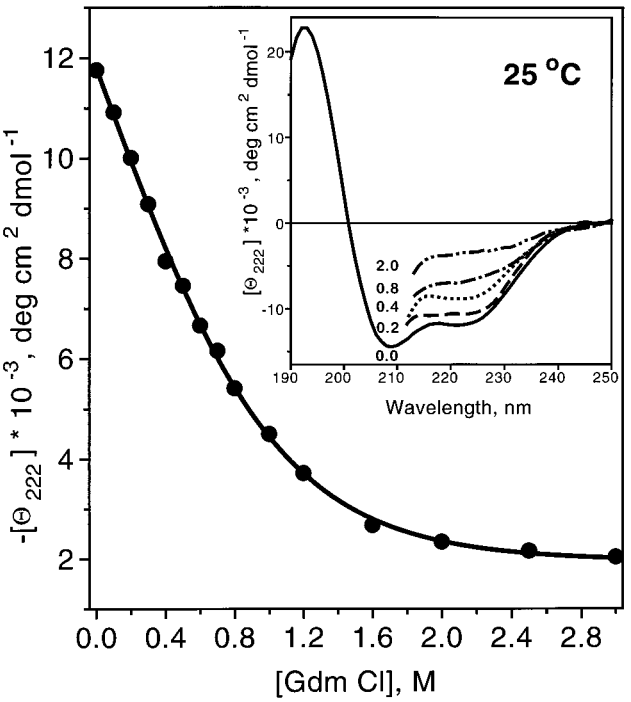

FIGURE 8: Gdm Cl unfolding of oligomeric apoC-1 monitored by CD at 222 nm. The data (shown in circles) were recorded at 25 °C from 100 μg/mL apoC-1 solution in 1 mM Na_2HPO_4, pH 7.5. The solid line illustrates the least-squares fit to the data by a sigmoidal function. Inset: CD spectra recorded at 25 °C from 100 μg/mL apoC-1 in 5 mM Na_2HPO_4, pH 7.5 at different Gdm Cl concentrations from 0 to 2 M (indicated on the lines). The spectra from Gdm Cl containing protein solutions are cut off at 212−215 nm because of the high UV absorption of the denaturant at short wavelengths.

resulting free energy estimate is $\Delta G_{H_2O}(25\ °C) = 1.8 \pm 1$ kcal/mol, with the error incorporating the uncertainty in the baseline determination and the fitting errors.

Guanidine Hydrochloride Unfolding of Oligomeric ApoC-1. In contrast to the chemical unfolding curves recorded from monomeric apoC-1 at 6.0−7.6 μg/mL concentrations, the Gdm Cl unfolding curve recorded at 0 and 25 °C from 100 μg/mL apoC-1 under otherwise identical solvent conditions lacks the pretransitional region (Figure 8). At 25 °C, the loss of the α-helical structure is readily detectable in the presence of only 0.2 M Gdm Cl (Figure 8, inset). This qualitatively agrees with the Gdm Cl unfolding data reported in ref *17* that was recorded from 200 μg/mL apoC-1 in neutral low-salt solution at 25 °C and also showed the absence of the plateau at low denaturant concentrations.

Thermodynamic Parameters for the ApoC-1 Monomer. Thermodynamic parameters determined from the CD data on the thermal and chemical unfolding of apoC-1 at 6.0−7.6 μg/mL concentrations, pH 7 (Figures 2, and 7) are summarized in Table 1. In the analysis, we assumed the thermodynamic equivalence of the heat-unfolded and Gdm HCl unfolded states, which has been established for numerous proteins on the basis of the identity of the thermodynamic values measured by thermal and chemical unfolding, even though the CD spectra for thermally and chemically unfolded states of these proteins are not identical (*31* and references therein). In the analysis of the unfolding data on apoC-1, we have used a minimalist two-state kinetic model, which is consistent with the presence of an isochromatic point in the spectra in Figure 1 and the apparent agreement between the measured van't Hoff enthalpy ΔH_v and the expected calorimetric enthalpy ΔH_{cal} for the heat unfolding. The most rigorous test for the two-state unfolding kinetics, which is the comparison of ΔH_v and ΔH_{cal} measured by differential scanning calorimetry (*32*), could not be done in this work because of the substantial self-association of apoC-1 in neutral low-salt solutions at the >1 mg/mL protein concentrations required for the calorimetric experiments. Therefore, the thermodynamic parameters reported in Table 1 are the effective (rather than calorimetric) enthalpy ΔH, the apparent free energy of stabilization ΔG, and the apparent heat capacity increment ΔC_p.

For an equilibrium two-state transition with the constant heat capacity increment $\Delta C_p(T)$, the value of ΔC_p can be estimated from the Gibbs−Helmholtz equation:

$$\Delta G(T) = \Delta H_v(T_m)(1 - T/T_m) - \Delta C_p(T_m - T + T\ln(T/T_m))$$

Using the values of $T_m = 50 \pm 3$ °C and $\Delta H(T_m) = 19 \pm 3$ kcal/mol measured in the thermal unfolding experiments, the first term in this equation can be estimated to be $\Delta H_v(T_m)(1 - T/T_m) = 2.9 \pm 0.5$ kcal/mol at $T = 0$ °C =273.15 K, and 1.5 ± 0.5 kcal/mol at $T = 25$ °C. Within the errors of their estimates, these values agree with the free energy of apoC-1 stabilization measured in the chemical unfolding experiments at 0 and 25 °C, $\Delta G(0\ °C) = 2.8 \pm 0.8$ kcal/mol and $\Delta G(25\ °C) = 1.8 \pm 1.0$ kcal/mol. Thus, the second term may not exceed the uncertainty in the determination of $\Delta G(T) - \Delta H_v(T_m)(1 - T/T_m)$ at 0 and 25 °C, which is ~1.5 kcal/mol. This provides an upper limit for $\Delta C_p \leq 0.3$ kcal/(mol·K) for apoC-1. This is small compared to $\Delta C_p = 0.6-0.9$ kcal/(mol·K) expected for a similar size globular protein, based on the partial heat capacity increments of 0.09−0.15 kcal/(g·K) reported for globular proteins (*27*, *32*, *33*). Small $\Delta C_p = d(\Delta H)/dT$ is also consistent with the linear character of the van't Hoff plot for monomeric apoC-1 (Figure 2B). Since the major contribution to ΔC_p arises from water ordering by apolar protein groups upon unfolding (*34*), the small ΔC_p inferred from the thermal and chemical unfolding of monomeric apoC-1 implicates the absence of a substantial hydrophobic core for the apoC-1 molecule in neutral low-salt solution.

DISCUSSION

Self-Association and Thermal Unfolding of ApoC-1. Sedimentation studies of apoC-1 showed that increasing protein concentration above 10 μg/mL at pH 7 and room temperature leads to self-association that is consistent with the monomer-dimer-trimer equilibrium with $K_{1,2} = 2.2$ L/g and $K_{1,3} = 9.2$ $(L/g)^2$ (*10*, *17*). Thus, in the protein concentration range 6−220 μg/mL used in this work, apoC-1 is present in the monomeric and/or dimeric forms. Self-association of apoC-1 has been shown to correlate with an increase in the α-helical content that was observed in ref 17 and in this work upon increasing apoC-1 concentration above 10 μg/mL at pH 7 and room temperature (curves 2−4 in Figure 4). Furthermore, the CD data of this work show that increasing the apoC-1 concentration above 10 μg/mL has a profound effect on the thermal unfolding. In addition to the heat unfolding that was detected under all experimental conditions explored

Table 1: Thermodynamic Parameters of ApoC-1 Monomer at pH 7[a]

parameter	value determined for apoC-1	expected value	
T_m	50 ± 3 °C		
$\Delta H(T_m)$	19 ± 3 kcal/mol	16−22 kcal/mol	enthalpy of unfolding of a ~17-residue α-helical structure, based on the values of 0.9−1.3 kcal/mol·residue measured for the unfolding of α-helical peptides in water (*29*)
ΔG(0 °C)	2.8 ± 0.8 kcal/mol		
ΔG(25 °C)	1.8 ± 1.0 kcal/mol	5−15 kcal/mol	measured for globular proteins (*27*, *32*)
		≤4.2 kcal/mol	reported for other exchangeable apolipoproteins, with an exception of the N-terminal domain of human apoE (*38*)
ΔC_p	≤0.3 kcal/(mol·K)	0.6−0.9 kcal/(mol·K)	expected of an ~6-kDa globular protein, based on the reported values of 0.09−0.15 kcal/(mol·g) (*29*, *30*)

[a] The melting temperature T_m and effective enthalpy $\Delta H(T_m)$ were determined from van't Hoff analysis of the thermal unfolding (Figure 2). The apparent free energies of stabilization ΔG(0 °C) and ΔG(25 °C) were determined from the chemical unfolding of monomeric apoC-1 (Figure 7). The apparent heat capacity increment ΔC_p was calculated by using the measured values of T_m, $\Delta H(T_m)$, and ΔG(0 °C) with the Gibbs−Helmholtz equation. The expected values that are based on the thermodynamic parameters reported for peptides, globular proteins, or other exchangeable apolipoproteins are given for comparison.

in this work, cold unfolding below 22 °C was observed at >10 μg/mL apoC-1, pH 7 (Figures 3, 4, and 6). Several lines of evidence indicate that this low-temperature transition reflects oligomer dissociation into stable monomers. (i) At pH 7, low-temperature unfolding is observed only under conditions where apoC-1 is known to form oligomers (20−220 μg/mL apoC-1, curves 2−4 in Figure 4) but not under conditions at which the protein is monomeric (6−7.6 μg/mL apoC-1, Figure 2). (ii) Low-temperature unfolding becomes more pronounced under conditions favoring self-association (such as high concentrations of apoC-1 (curves 3 and 4 in Figure 4) and Na_2HPO_4 (curve 2 in Figure 6)) and is abolished under conditions that are known to promote dissociation of apoC-1 oligomers (such as acidic pH (curve 1 in Figure 4) or the presence of Gdm Cl (curve 3 in Figure 6)). (iii) In contrast to the complete loss of the α-helical structure upon heating to 90 °C, at least 30% α-helical content is retained upon cooling to −10 °C (Figures 3 and 4), which is comparable to the α-helical content observed in monomeric apoC-1 below 22 °C (Figures 1 and 2). (iv) Substantial reduction in the intensity of the characteristic CD bands at 193, 208, and 222 nm upon cooling of oligomeric apoC-1 from 22 to −8 °C (Figure 3B), coincident ellipticity changes at various wavelengths, and the sigmoidal shape of the thermal unfolding curves at T < 22 °C (Figure 4, insert) indicate that the spectral changes observed at low temperatures reflect cooperative partial unfolding of the α-helical structure in oligomeric apoC-1. These results clearly indicate that the low-temperature transition reflects the unfolding of the additional α-helices that form upon apoC-1 self-association at ~22 °C, while the high-temperature transition reflects a complete unfolding of the apoC-1 molecule.

Structural Characteristics of the ApoC-1 Molecule. The CD data presented in this work suggest that the secondary structure of the apoC-1 monomer in neutral low-salt solutions at ≤22 °C is composed of a ~17-residue α-helical "nucleus" which undergoes a low-cooperativity unfolding between about 22 and 80 °C. Comparison with the melting of isolated α-helices in water (which is characterized by ≤20 residues in a cooperative unit (*29*, *32*, and references therein)) suggests that tertiary interactions may not play a large role in stabilizing the α-helical structure in apoC-1. This is consistent with the absence of a substantial hydrophobic core in the apoC-1 monomer inferred from the small heat capacity increment ΔC_p, and with the enhanced monomer stability measured at 0 °C compared to that at 25 °C (Table 1). The α-helical structure in the apoC-1 molecule may be stabilized by enthalpic interactions, such as intrahelical salt links between oppositely charged residues located 3−4 positions apart. The sequence of apoC-1 suggests that the majority of the charged residues from the predicted α-helical regions (including Asp9, Lys10, Lys12, Glu13, Glu19, Asp20, Lys21, Arg23, Glu24, Arg28, Lys30, Glu33, Lys37, Arg39, Glu40, Glu44, and Lys48) may potentially be involved in intrahelical salt links. The importance of such salt links for the conformation and stability of the N-terminal domain of normal and mutant human apoE has been demonstrated by X-ray crystallography (*14*, *35*). Disruption of such salt links upon protonation of acidic groups in apoC-1 is consistent with the reduced α-helical content and the loss of the heat unfolding cooperativity observed upon lowering the pH from 7 to 3.7 (Figures 1 and 5 compared to Figure 4).

The results of this and the earlier studies suggest that apoC-1 possesses some of the structural and thermodynamic characteristics of the molten globule, such as a high propensity to self-associate (*17*), broad thermal unfolding (this work), low denaturing concentrations of Gdm Cl (17, this work), relatively low values of ΔG(25 °C) and ΔH (this work), and low a value of ΔC_p that suggests the absence of a well-defined hydrophobic core structure (this work). However, the secondary structure in the apoC-1 monomer is <45% folded, compared to the typical molten globule whose secondary structure constitutes ~80% of that in the native state (*20*, *21*). Thus, in contrast to the monomeric lipid-free apoA-1 that is >60% α-helical, the lipid-free apoC-1 molecule cannot be termed "molten globule" since most of its secondary structure is disordered. This suggests that, in contrast to the tertiary structure adaptability of molten globular apoA-1, the secondary structure adaptability of apoC-1 (which can undergo more than a 2-fold increase in the α-helical content upon self-association and lipid binding (*10*, *17*)) is essential for the apoC-1 function as an exchangeable apolipoprotein.

In contrast to monomeric apoC-1 that is more stable at 0 °C than at 25 °C (Figure 7, Table 1), low-order oligomers that form at pH 7 and protein concentrations above 10 μg/mL are most stable at room temperature and dissociate not only upon heating but also upon cooling from ~22 °C (Figures 4 and 6). This indicates a substantial contribution of hydrophobic interactions to the stability of apoC-1

oligomers; a decrease in the hydrophobic interactions at low temperature leads to oligomer dissociation. Similarly, complete loss of the secondary structure upon cold denaturation reported for a variety of globular proteins (reviewed in *36*) and apoA-2 (*19*, *37*) indicates the importance of hydrophobic interactions for the stability of the native protein conformation.

CD spectroscopic observation of the low-temperature oligomer dissociation in this work was facilitated by an increased α-helical content in apoC-1 oligomers compared to that in monomers. Formation of these additional α-helices has apparently no large effect on the stability of the initial ∼17-residue α-helical structure in apoC-1. Indeed, the small high-temperature shifts in the melting curves observed upon increasing protein concentration (curves 2−4 in Figure 4) may be a consequence of Le Chatelier's principle rather than the enhanced oligomer stability. Moreover, close proximity between the high- and low-temperature transitions (Figures 4 and 6) and the absence of a plateau in the Gdm Cl unfolding curve recorded from oligomeric apoC-1 at 100−200 μg/mL concentrations, pH 7, 25 °C (Figure 8 and ref *17*) indicate only marginal stability for the low-order apoC-1 oligomers in neutral low-salt solutions. This marginal oligomer stability, along with the partially ordered secondary structure of the monomer in neutral low-salt solutions, suggests that apoC-1 transfer in plasma may be mediated via complexes with other apolipoproteins (such as apoC-2 and apoC-3) and/or lipids.

The results of this work provide a basis for the future structural and thermodynamic analysis of site-specific mutants of apoC-1 that can be obtained by solid-state synthesis. Such an analysis should make it possible to (i) identify the residues forming the initial ∼17−residue α-helical "nucleus" in the apoC-1 molecule and the intramolecular interactions stabilizing these helices; (ii) define additional α-helices that form upon apoC-1 self-association and are stabilized by interhelical interactions of a largely hydrophobic nature; and (iii) obtain apoC-1 mutants of enhanced structural stability and utilize these mutants for the analysis of the energetic structure−function relationship in apolipoproteins.

ACKNOWLEDGMENT

We thank Ann Tercyak, Cheryl England, and Michael Gigliotti for protein isolation and purification.

REFERENCES

1. Schaefer, E. J., Eisenberg, S., and Levy, R. I. (1978) *J. Lipid Res. 19*, 667−687.
2. Windler, E., and Havel, R. J. (1985) *J. Lipid Res. 26*, 556−565.
3. Fidge, N. H., and Nestel, P. J. (1986) *Methods Enzymol. 129*, 443−456.
4. Soutar, A. K., Garner, C. W., Baker, H. N., Sparrow, J. T., Jackson, R. L., Gotto, A. M., Jr., and Smith, L. C. (1975) *Biochemistry 14*, 3057−3064.
5. Streyer, E., and Kostner, G. M. (1988) *Biochim. Biophys. Acta 958*, 484−491.
6. Mahley, R. W., Innerarity, T. L., Rall, S. C., and Weisgraber, K. H. (1984) *J. Lipid Res. 25*, 1277−1294.
7. Hodis, H. N., Mack, W. J., Azen, S. P., et al. (1994) *Circulation 90*, 42−49.
8. Sehayek, E., and Eisenberg, S. (1991) *J. Biol. Chem. 266*, 18259−18267.
9. Weisgraber, K. H., Mahley, R. W., Kowal, R. W., Brown, M. S., and Goldstein, J. L. (1990) *J. Biol. Chem. 265*, 22453−22459.
10. Osborne, J. C., Jr., and Brewer, H. B., Jr. (1977) *Adv. Protein Chem. 31*, 253−337.
11. Osborne, J. C., Jr., Lee, N. S., and Powell, G. M. (1986) *Methods Enzymol. 128*, 375−387.
12. Segrest, J. P., Jones, M. K., De Loof, H., Brouilette, C. G., Venkatachalapathi, Y. V., and Anantharamaiah, G. M. (1992) *J. Lipid Res. 33*, 141−166.
13. Breiter, D. R., Kanost, M. R., Benning, M. M., Wesenberg, G., Law, J. H., Wells, M. A., Rayment, I., and Holden, H. M. (1991) *Biochemistry 30*, 603−608.
14. Wilson, C., Wardell, M. R., Weisgraber, K. H., Mahley, R. W., and Agard, D. A. (1991) *Science 252*, 1817−1822.
15. Weisgraber, K. H., Newhouse, Y. M., and McPherson, A. (1994) *J. Mol. Biol. 236*, 382−384.
16. Rozek, A., Buchko, G. W., Kanda, P., and Gushley, R. J. (1997) *Protein Sci. 6*, 1858−1868.
17. Osborne, J. C., Jr., Bronzert, T. J., and Brewer, H. B., Jr. (1977) *J. Biol. Chem. 252*, 5756−5760.
18. Gursky, O., and Atkinson, D. A. (1996) *Proc. Natl. Acad. Sci. USA 93*, 2991−2995.
19. Gursky, O., and Atkinson, D. A. (1996) *Protein Sci. 5*, 1874−1882.
20. Ptitzyn, O. B. (1995) *Adv. Protein Chem. 47*, 83−229.
21. Haynie, D. T., and Freire, E. (1993) *Proteins 1*, 16−22.
22. Jackson, R. L., and Holdsworth, G. (1986) *Methods Enzymol. 128*, 288−297.
23. Markwell, M. A. K., Haas, S. M., Bieber, L. L., and Tolberg, N. E. A. (1985) *Anal. Biochem. 87*, 206−210.
24. Greenfield, N., and Fasman, G. D. (1969) *Biochemistry 8*, 4108−4116.
25. Chen, Y.-H., Yang, J. T., and Martinez, H. M. (1972) *Biochemistry 11*, 1420−1431.
26. Mao, D., and Wallace, B. A. (1984) *Biochemistry 23*, 2677−2673.
27. Pace, C. N., Shirley, B. A., and Thomson, J. A. (1989) *Protein Structure* pp 311−330, IRL Press, New York.
28. Carra, J. H., Anderson, E. A., and Privalov, P. L. (1994) *Protein Sci. 3*, 944−951.
29. Scholtz, J. M., Marqusee, S., Baldwin, R. L., York, E. J., Stewart, J. M., Santoro, M., and Bolen, D. W. (1991) *Proc. Natl. Acad. Sci. U.S.A. 88*, *2854*−2858.
30. Marky, L. A., and Breslauer, K. J. (1987) *Biopolymers 26*, 1601−1620.
31. Scholtz, J. M. (1995) *Protein Sci. 4*, 35−53.
32. Privalov, P. L. (1979) *Adv. Protein Chem. 35*, 1−104.
33. Privalov, P. L., Tiktopulo, E. I., Venyaminov, S. Yu., Griko, Yu. V., Makhatadze, G. I., and Khechinashvili, N. N. (1989) *J. Mol. Biol. 205*, 737−750.
34. Makhatadze, G. I., and Privalov, P. L. (1990) *J. Mol. Biol. 213*, 385−391.
35. Wilson, C., Mau, T., Weisgraber, K. H., Wardell, M. R., Mahley, R. W., and Agard, D. A. (1994) *Structure 2*, 713−718.
36. Privalov, P. L. (1990) *Crit. Rev. Biochem. Mol. Biol. 25*, 281−305.
37. Gwynne, J., Palumbo, G., Osborne, H. C., Jr., Brewer, H. B., Jr., and Edelhoch, H. (1975) *Arch. Biochem. Biophys. 170*, 204−212.
38. Wetterau, J. R., Aggerbeck, L. P., Rall, S. C., Jr., and Weisgraber, K. H. (1988) *J. Biol. Chem. 263*, 6240−6248.

BI971801Q